Forest Chemicals Revew
www.forestchemicalsreview.com
ISSN: 1520-0191
July-August 2021 Page No. 783-806
Article History: Received: 12 May 2021 Revised: 25 June 2021 Accepted: 22 July 2021 Publication: 31 August 2021

Theoretical Analysis Method of Moiré Display Based on Microlens Array with Regular Hexagonal Aperture and Honeycomb Arrangement

Linyi Chen[1], Qiao Chen[1*], Liyu Liao[2], Guangxue Chen[3]
[1]School of Communication Engineering, Shenzhen Polytechnic, Shenzhen, China
[2]YUTO Institute, Shenzhen YUTO Packaging Technology Co., Ltd., Shenzhen, China
[3]School of Light Industry and Engineering, South China University of Technology, Guangzhou, China
* Corresponding Author.

Abstract:

The naked-eye 3D printing technology based on microlens array can achieve the naked-eye 3D display effect within 360° full angle without the help of glasses, helmet and other visual aids or observation skills. It can significantly improve the information display level, interest and anti-counterfeiting performance of the product, increase the visual impact and sensory experience of the product, and greatly enhance the added value of the product, which has significant engineering application values in the fields of printing, publishing, anti-counterfeiting, decoration, display, etc. However, the naked-eye 3D printing technology based on microlens array currently lacks the necessary theoretical analysis method of moiré display, which embody in the following aspect: the existing methods only focus on the array magnification features of moiré pattern, ignoring the spatial direction features and unit magnification features of moiré pattern. In this paper, on the basis of the existing geometric transformation method, a moiré display theoretical analysis method was proposed for microlens array with regular hexagonal aperture and honeycomb arrangement, which gave consideration to the imaging characteristics of moiré pattern, such as periodic amplification, unit amplification and spatial direction. The mathematical relationship between the period, direction angle, period magnification, unit magnification of moiré pattern and the period of microlens array, the period of micrographics array, as well as the superposition angle of them were derived in detail. The two typical cases were selected, and the theoretical and experimental values of the period, the direction angle, the period magnification and the unit magnification of moiré pattern were calculated and tested respectively. The differences between the theoretical and experimental values were then compared. The results show that the deviation rates between the experimental and theoretical values of the period, the direction

Forest Chemicals Revew
www.forestchemicalsreview.com
ISSN: 1520-0191
July-August 2021 Page No. 783-806
Article History: Received: 12 May 2021 Revised: 25 June 2021 Accepted: 22 July 2021 Publication: 31 August 2021

angle, the period magnification and the unit magnification are all less than 2% in two typical cases, which verified the effectiveness of the proposed moiré display theoretical analysis method.

Keywords*: Moiré optical effect, Microlens array, Micrographics array, Naked-eye 3D display.*

I. INTRODUCTION

The naked-eye 3D printing technology based on microlens array can achieve the naked-eye 3D display effect within 360^{o} full angle without the help of glasses, helmet and other visual aids or observation skills. It can significantly improve the information display level, interest and anti-counterfeiting performance of the product, increase the visual impact and sensory experience of the product, and greatly enhance the added value of the product, which has significant engineering application values in the fields of printing, publishing, anti-counterfeiting, decoration, display, and represents the development direction of hi-end packaging and printing industry [1]. Fig 1 shows the schematic diagram of the principle of naked-eye 3D imaging based on microlens array.

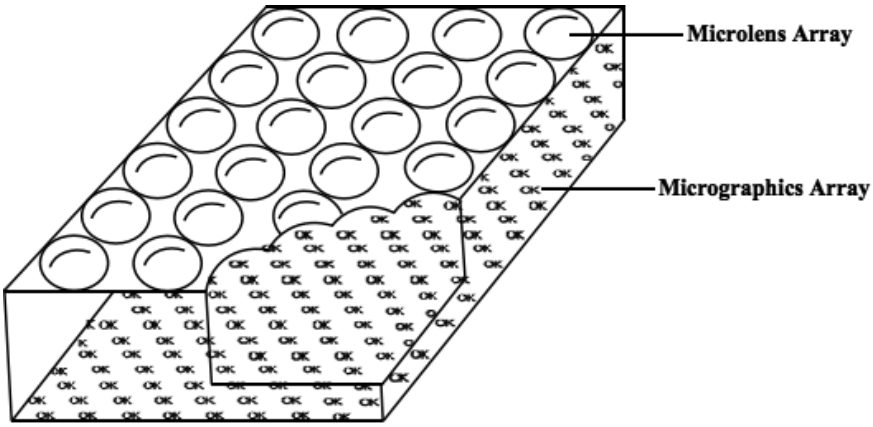

Fig 1: Schematic diagram of the principle of naked-eye 3D imaging based on microlens array.

In 1994, British scholar M. Hutley [2] first proposed the concept of moiré amplifier, pointed out that moiré amplifier is a kind of optical variable device composed of periodic microlens array and micrographics array, and preliminarily studied the basic properties of moiré amplifier. Subsequently, relevant researchers at home and abroad [3-10] conducted in-depth research on moiré amplifier, and further extended the structural definition of moiré amplifier, so that the basic structure of moiré amplifier is extended to aperiodic structure rather

Forest Chemicals Revew
www.forestchemicalsreview.com
ISSN: 1520-0191
July-August 2021 Page No. 783-806
Article History: Received: 12 May 2021 Revised: 25 June 2021 Accepted: 22 July 2021 Publication: 31 August 2021

than limited to microlens array.

The combination of microlens array and micrographics array can produce moiré optical effect. The moiré optical effect based on microlens array is the result of integrated imaging of micrographics by multiple microlenses. Microlens array has two important features for moiré imaging of micrographics array: moiré amplification feature and moiré depth of field feature. Therefore, when the microlens array and the micrographics array are overlapped with each other, under the resolution limit of the human eye, the observer can directly see the moiré pattern with a certain magnification and a certain depth of field with the naked-eye based on the binocular parallax principle. Fig 2 and Fig 3 show schematic diagrams of moiré amplification effect based on microlens array and moiré depth of field effect based on microlens array, respectively.

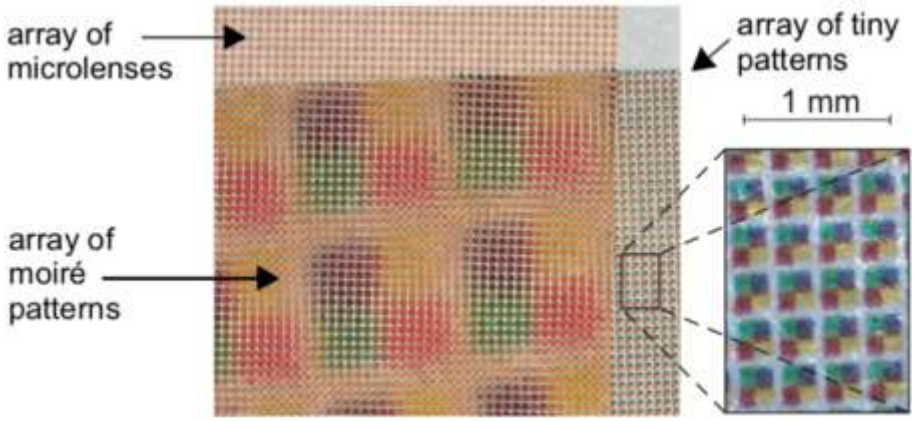

Fig 2: Schematic diagram of moiré amplification effect based on microlens array

Forest Chemicals Revew
www.forestchemicalsreview.com
ISSN: 1520-0191
July-August 2021 Page No. 783-806
Article History: Received: 12 May 2021 Revised: 25 June 2021 Accepted: 22 July 2021 Publication: 31 August 2021

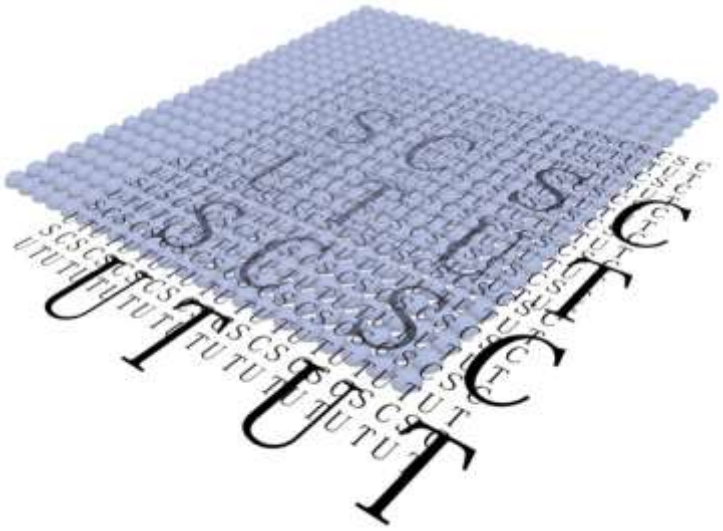

Fig 3: Schematic diagram of moiré depth of field effect based on microlens array

The display effect of moiré pattern based on microlens array is closely related to the period, spatial arrangement and superposition angle of microlens array and micrographics array. In this paper, the spatial arrangement of microlens array is honeycomb arrangement, and the microlens unit is regular hexagonal aperture. The spatial layout of micrographics array is also cellular layout; the micrographics unit can be hexagonal star, circle or other pattern shapes, the circle shape is chosen here. As shown in Fig 4, it is the schematic diagram of the structure and spatial arrangement of microlens array and micrographics array.

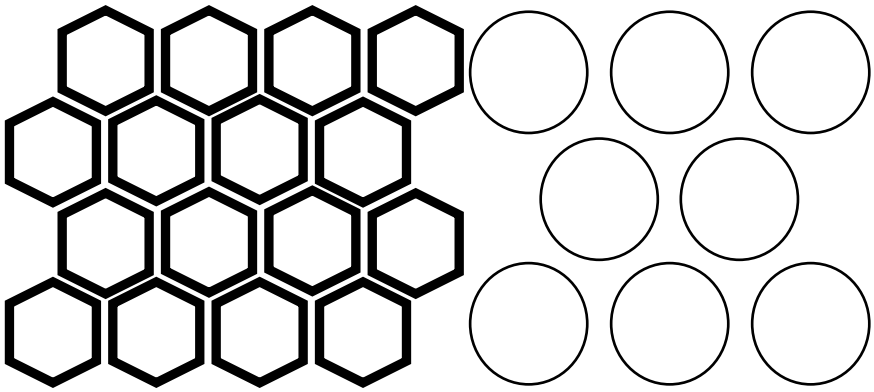

Fig 4: Schematic diagram of the structure and spatial arrangement of microlens array and micrographics array

According to the relevant literature research, the naked-eye 3D printing technology based

Forest Chemicals Revew
www.forestchemicalsreview.com
ISSN: 1520-0191
July-August 2021 Page No. 783-806
Article History: Received: 12 May 2021 Revised: 25 June 2021 Accepted: 22 July 2021 Publication: 31 August 2021

on microlens array currently lacks the necessary theoretical analysis method of moiré display, which embody in the following aspects: the existing methods only focus on the array amplification characteristics of moiré pattern, and extremely simplify the periodic formula of moiré pattern as $T = (T_1T_2)/|T_1 - T_2|$ (where T, T_1, T_2 are moiré pattern array period, microlens array period and micrographics array period respectively), ignoring the spatial direction features and unit magnification features of moiré pattern. In addition, no moiré display theoretical analysis methods for hexagonal aperture and honeycomb microlens array has been found and reported. Isaac Amidror pointed out in his monograph 'the theory of the moiré phenomenon' that moiré fringes are the result of periodic modulation of light by two or more periodic or aperiodic repetitive structural objects [11]. Presently, there are three theories to explain the formation mechanism of moiré fringes: the shadow imaging theory, the diffraction interference theory and the Fourier transform theory [12-15]. Based on the above formation mechanism of moiré fringe, there are three common and widely used moiré fringe analysis methods, namely, the indicial equations method, the geometric transformation method and the frequency spectrum method based on Fourier transform [16-18]. In this paper, the theoretical analysis method of moiré display for regular hexagonal aperture and honeycomb microlens array was creatively put forward based on the geometric transformation method, and the mathematical relationship between the period, direction angle, periodic magnification, unit magnification and the period of microlens array, the period of micrographics array and their superposition angle was deduced.

II. THEORETICAL ANALYSIS METHOD OF MOIRE DISPLAY BASED ON MICROLENS ARRAY

In theory, the microlens array with the honeycomb arrangement and regular hexagonal aperture, the micrographics array with the honeycomb arrangement and circular unit in Fig 4 can be regarded as the superposition of a group of double cluster line gratings, as shown in Fig 5. On the left are two clusters of line gratings representing microlens array, and on the right are two clusters of line gratings representing micrographics array. The moiré display effect of microlens array with the honeycomb arrangement and regular hexagonal aperture on the corresponding micrographics array can be simulated by the dynamic superposition between two groups of double cluster line gratings. The moiré display simulation analysis of two groups of double cluster line gratings superimposed at different angles can actually be regarded as the mutual superposition of four cluster line gratings as shown in Fig 6. Among them, I and II are the two clusters of line gratings constituting the microlens array respectively, and III and IV are the two clusters of line gratings constituting the micrographics array respectively.

Forest Chemicals Revew
www.forestchemicalsreview.com
ISSN: 1520-0191
July-August 2021 Page No. 783-806
Article History: Received: 12 May 2021 Revised: 25 June 2021 Accepted: 22 July 2021 Publication: 31 August 2021

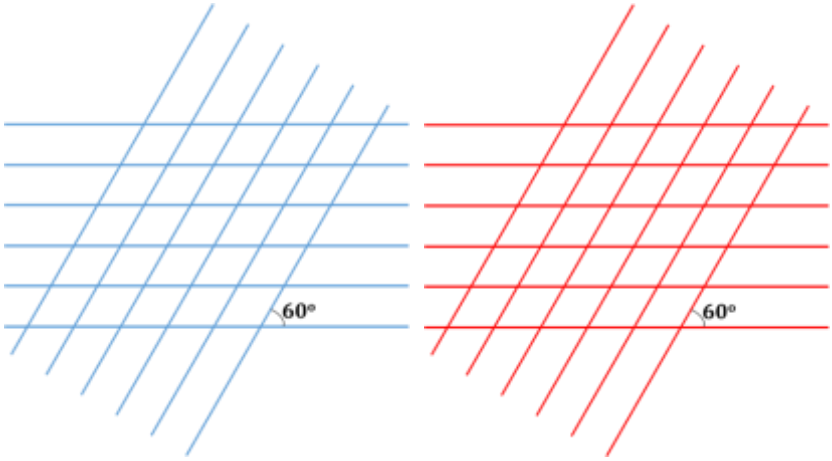

Fig 5: Two groups of double cluster line gratings of microlens array and micrographics array and their superposition relationship

When the microlens array and the micrographics array overlap with each other at a certain included angle (it is assumed here that the spatial position of the microlens array remains unchanged, and the micrographics array rotates θ clockwise as a whole), according to the spatial arrangement of the microlens array and the micrographics array itself, the included angle between I and II, and the included angle between III and IV are always 60^{o}, that is, the mutual superposition between I and II, III and IV will never produce the moiré pattern. However, I will overlap with III and IV respectively to produce two groups of moiré patterns; II will overlap with III and IV to produce two groups of moiré patterns. The moiré patterns generated by the superposition of I and III, I and IV, II and III, and II and IV are shown respectively in Fig 7.

Forest Chemicals Revew
www.forestchemicalsreview.com
ISSN: 1520-0191
July-August 2021 Page No. 783-806
Article History: Received: 12 May 2021 Revised: 25 June 2021 Accepted: 22 July 2021 Publication: 31 August 2021

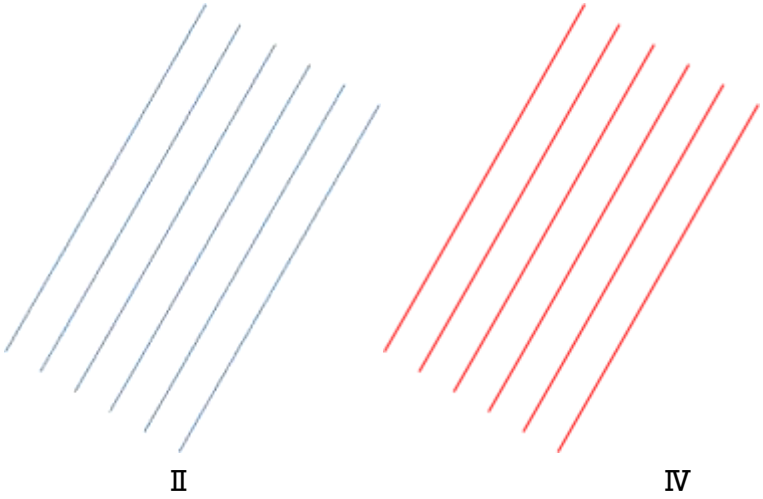

Fig 6: Four cluster line grating of microlens array and micrographics array

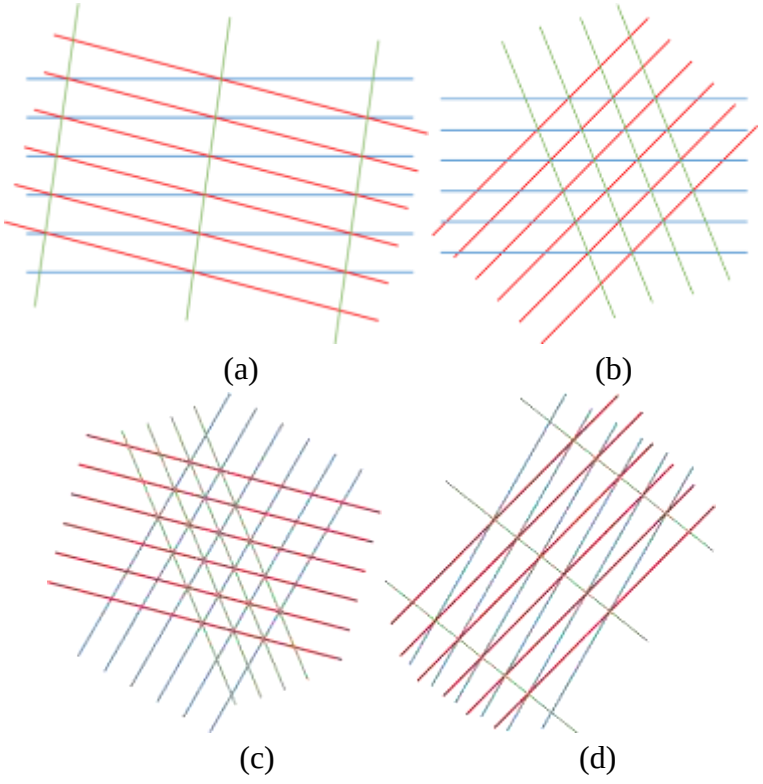

Fig 7: Schematic diagram of moiré fringe pattern generated by the superposition of two groups of double cluster line gratings, in which blue is the grating line cluster of the microlens array, red is the grating line cluster of the micrographics array, and green is the grating line cluster of the moiré fringe pattern: (a) the moiré fringe pattern formed by the superposition of I and III; (b) the moiré fringe pattern formed by the superposition of I and IV; (c) the moiré fringe pattern formed

Forest Chemicals Revew
www.forestchemicalsreview.com
ISSN: 1520-0191
July-August 2021 Page No. 783-806
Article History: Received: 12 May 2021 Revised: 25 June 2021 Accepted: 22 July 2021 Publication: 31 August 2021

by the superposition of II and III; (d) the moiré fringe pattern formed by the superposition of II and IV

2.1 Period and Direction Angle of Moiré Pattern

Suppose the periods of microlens array and micrographics array are d_1 and d_2 respectively, and the micrographics array rotates θ clockwise as a whole, $0^o \leq \theta \leq 180^o$. The moiré pattern formed by the superposition of I and III has a period of S_1 and a direction angle of φ_1; the moiré pattern formed by the superposition of I and IV has a period of S_2 and a direction angle of φ_2; the moiré pattern formed by the superposition of II and III has a period of S_3 and a direction angle of φ_3; The moiré pattern formed by the superposition of II and IV has a period of S_4 and a direction angle of φ_4.

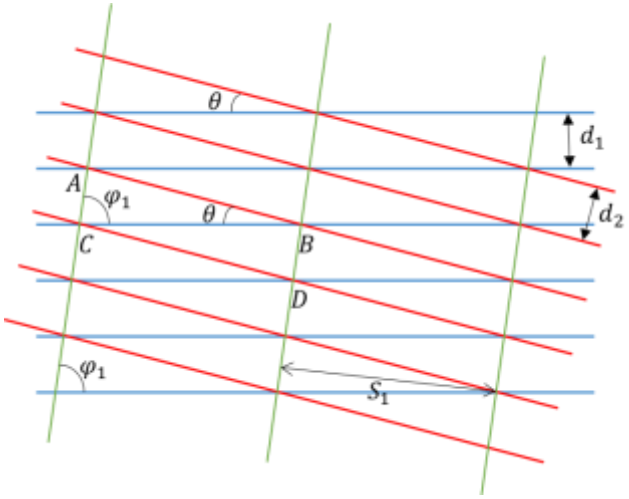

Fig 8: Calculation schematic diagram of moiré pattern formed by superposition of I and III

As shown in Fig 8, for the moiré pattern formed by the superposition of I and III, the period of line grating cluster I is d_1, the period of line grating cluster II is d_2, and the included angle between the two groups of line grating clusters is θ.

It can be seen from Fig 8:

$$\overline{BC} * d_1 = \overline{AB} * d_2 = \overline{CD} * d_2 = \overline{AC} * S_1 = \overline{BD} * S_1 \quad (1)$$

$$\overline{AC}^2 = \overline{AB}^2 + \overline{BC}^2 - 2\overline{AB} * \overline{BC} * cos\,\theta \quad (2)$$

$$\overline{AB}^2 = \overline{AC}^2 + \overline{BC}^2 - 2\overline{AC} * \overline{BC} * cos\,\varphi_1 \quad (3)$$

Forest Chemicals Revew
www.forestchemicalsreview.com
ISSN: 1520-0191
July-August 2021 Page No. 783-806
Article History: Received: 12 May 2021 Revised: 25 June 2021 Accepted: 22 July 2021 Publication: 31 August 2021

It can be obtained from equations (1), (2) and (3):

$$S_1 = \frac{d_1 d_2}{\sqrt{d_1^2 + d_2^2 - 2d_1 d_2 \cos\theta}} \tag{4}$$

$$\varphi_1 = arc\cos\frac{\mathrm{d_2} - \mathrm{d_1}\cos\ \theta}{\sqrt{\mathrm{d_1^2} + \mathrm{d_2^2} - 2\mathrm{d_1 d_2}\cos\ \theta}} \tag{5}$$

As shown in Fig 9, for the moiré pattern formed by the superposition of I and IV:

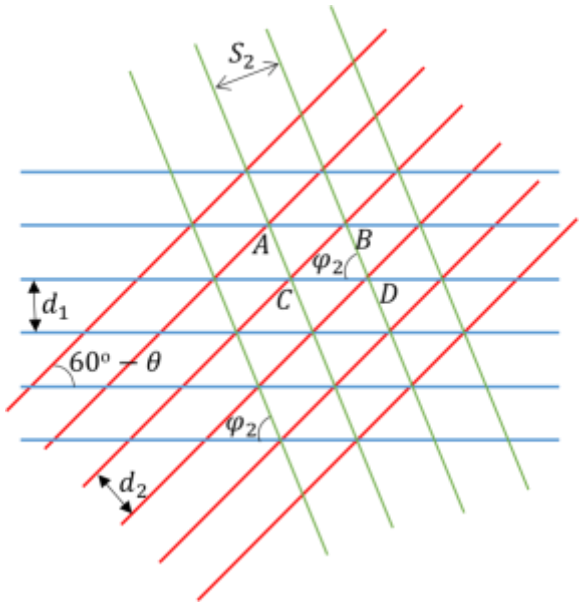

Fig 9: Calculation schematic diagram of moiré pattern formed by superposition of I and IV

It can be seen from Fig. 9:

$$\overline{AB} * d_1 = \overline{CD} * d_1 = \overline{BC} * d_2 = \overline{BD} * S_2 = \overline{AC} * S_2 \tag{6}$$

$$\overline{AC}^2 = \overline{AB}^2 + \overline{BC}^2 - 2\overline{AB} * \overline{BC} * cos(60^o - \theta) \tag{7}$$

$$\overline{BC}^2 = \overline{BD}^2 + \overline{CD}^2 - 2\overline{BD} * \overline{CD} * cos\,\varphi_2 \tag{8}$$

It can be obtained from equations (6), (7) and (8):

Forest Chemicals Revew
www.forestchemicalsreview.com
ISSN: 1520-0191
July-August 2021 Page No. 783-806
Article History: Received: 12 May 2021 Revised: 25 June 2021 Accepted: 22 July 2021 Publication: 31 August 2021

$$S_2 = \frac{d_1 d_2}{\sqrt{d_1^2 + d_2^2 - 2d_1 d_2 \cos(60^o - \theta)}} \tag{9}$$

$$\varphi_2 = arc\cos\frac{d_2 - d_1\cos(60^o - \theta)}{\sqrt{d_1^2 + d_2^2 - 2d_1 d_2 \cos(60^o - \theta)}} \tag{10}$$

As shown in Fig 10, for the moiré pattern formed by the superposition of II and III:

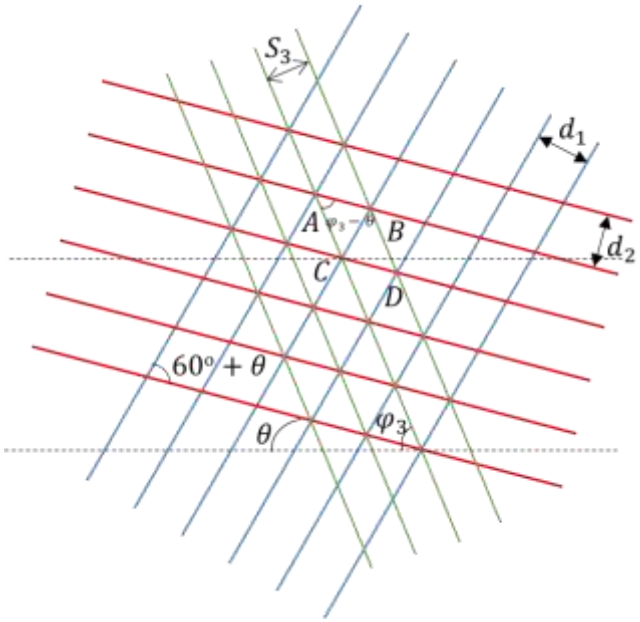

Fig 10: Calculation schematic diagram of moiré pattern formed by superposition of II and III

It can be seen from Fig 10:

$$\overline{BC} * d_1 = \overline{AB} * d_2 = \overline{CD} * d_2 = \overline{AC} * S_3 = \overline{BD} * S_3 \tag{11}$$

$$\overline{AC}^2 = \overline{AB}^2 + \overline{BC}^2 - 2\overline{AB} * \overline{BC} * \cos(60^o + \theta) \tag{12}$$

$$\overline{BC}^2 = \overline{AB}^2 + \overline{AC}^2 - 2\overline{AB} * \overline{AC} * \cos(\varphi_3 - \theta) \tag{13}$$

It can be obtained from equations (11), (12) and (13):

Forest Chemicals Revew
www.forestchemicalsreview.com
ISSN: 1520-0191
July-August 2021 Page No. 783-806
Article History: Received: 12 May 2021 Revised: 25 June 2021 Accepted: 22 July 2021 Publication: 31 August 2021

$$S_3 = \frac{d_1 d_2}{\sqrt{d_1^2 + d_2^2 - 2d_1 d_2\, cos(60^o + \theta)}} \tag{14}$$

$$\varphi_3 = arc\, cos \frac{d_1 - d_2\, cos(60^o + \theta)}{\sqrt{d_1^2 + d_2^2 - 2d_1 d_2\, cos(60^o + \theta)}} + \theta \tag{15}$$

As shown in Fig 11, for the moiré pattern formed by the superposition of II and IV:

$$\overline{AC} * d_1 = \overline{BD} * d_1 = \overline{BC} * d_2 = \overline{AB} * S_4 = \overline{CD} * S_4 \tag{16}$$

$$\overline{AB}^2 = \overline{AC}^2 + \overline{BC}^2 - 2\overline{AC} * \overline{BC} *\ cos\,\theta \tag{17}$$

$$\overline{BC}^2 = \overline{AB}^2 + \overline{AC}^2 - 2\overline{AB} * \overline{AC} * cos(120^o - \varphi_4) \tag{18}$$

It can be obtained from equations (16), (17) and (18):

$$S_4 = \frac{d_1 d_2}{\sqrt{d_1^2 + d_2^2 - 2d_1 d_2\, cos\,\theta}} \tag{19}$$

$$\varphi_4 = 120^o - arc\, cos \frac{d_2 - d_1\, cos\,\theta}{\sqrt{d_1^2 + d_2^2 - 2d_1 d_2\, cos\,\theta}} \tag{20}$$

Forest Chemicals Revew
www.forestchemicalsreview.com
ISSN: 1520-0191
July-August 2021 Page No. 783-806
Article History: Received: 12 May 2021 Revised: 25 June 2021 Accepted: 22 July 2021 Publication: 31 August 2021

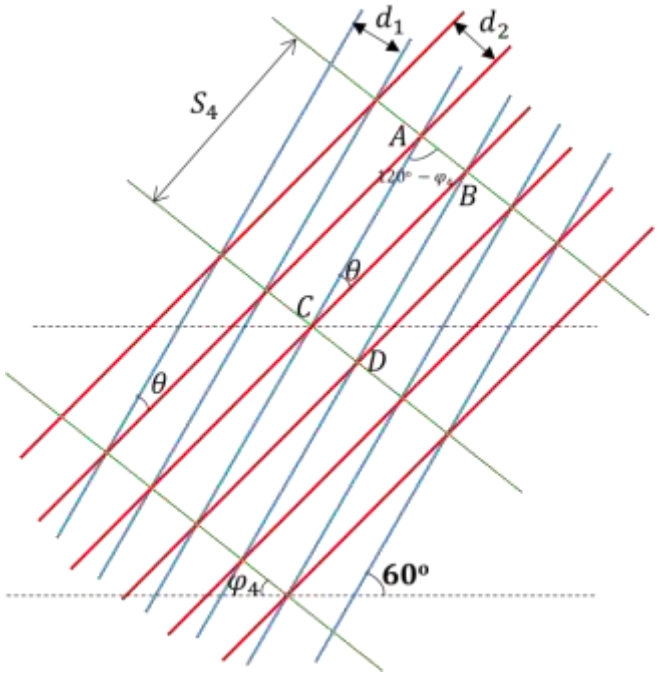

Fig 11: Calculation schematic diagram of moiré pattern formed by superposition of II and IV

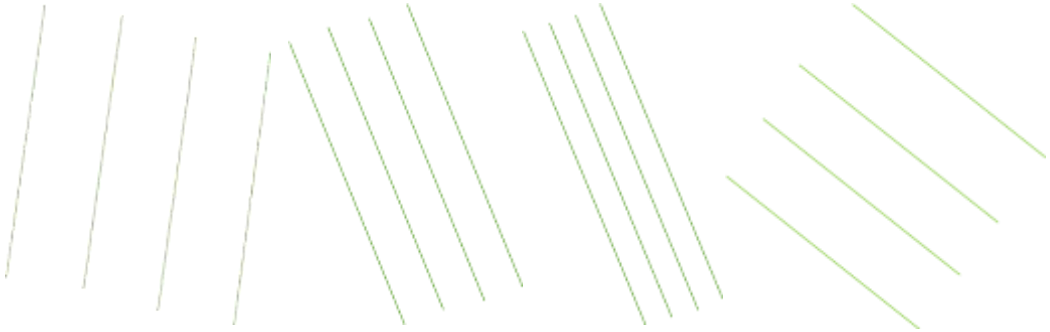

Fig 12: Schematic diagram of spatial distribution of four groups of moiré pattern, from left to right are moiré pattern 1, moiré pattern 2, moiré pattern 3 and moiré pattern 4 respectively

Through the above derivation, the calculation formulas of the period and direction angle of the moiré pattern generated by the superposition of I and III, I and IV, II and III, and II and IV are obtained, which are successively called moiré pattern 1, moiré pattern 2, moiré pattern 3 and moiré pattern 4, as shown in Fig 12.

For the convenience of expression, we introduce vectors $\overrightarrow{S_{\varphi_1}}, \overrightarrow{S_{\varphi_2}}, \overrightarrow{S_{\varphi_3}}, \overrightarrow{S_{\varphi_4}}$, which represent moiré pattern 1, moiré pattern 2, moiré pattern 3 and moiré pattern 4 respectively.

Forest Chemicals Revew
www.forestchemicalsreview.com
ISSN: 1520-0191
July-August 2021 Page No. 783-806
Article History: Received: 12 May 2021 Revised: 25 June 2021 Accepted: 22 July 2021 Publication: 31 August 2021

Then their period size $S_1,\ S_2,\ S_3,\ S_4$ and direction angle $\varphi_1,\ \varphi_2,\ \varphi_3,\ \varphi_4$ satisfy:

$$\left|\overrightarrow{S_{\varphi_1}}\right| = S_1, \left|\overrightarrow{S_{\varphi_2}}\right| = S_2, \left|\overrightarrow{S_{\varphi_3}}\right| = S_3, \left|\overrightarrow{S_{\varphi_4}}\right| = S_4 \tag{21}$$

$\varphi_1,\ \varphi_2,\ \varphi_3,\ \varphi_4$ are the angles between the vector $\overrightarrow{S_{\varphi_1}}, \overrightarrow{S_{\varphi_2}}, \overrightarrow{S_{\varphi_3}}, \overrightarrow{S_{\varphi_4}}$ and the positive or negative axis, respectively, and $0^o \le \varphi_1, \varphi_2, \varphi_3, \varphi_4 \le 90^o$.

Assuming $\overrightarrow{S_\varphi}$ represents the moiré pattern generated by the superposition of microlens array and micrographics array, its period size and direction angle can be expressed as:

$$S = \left|\overrightarrow{S_\varphi}\right| = max(\left|\overrightarrow{S_{\varphi_1}}\right|, \left|\overrightarrow{S_{\varphi_2}}\right|, \left|\overrightarrow{S_{\varphi_3}}\right|, \left|\overrightarrow{S_{\varphi_4}}\right|) = max(S_1, S_2, S_3, S_4) \tag{22}$$

When the period size S is determined, the direction angle φ is the direction angle corresponding to the maximum value in S_1, S_2, S_3, S_4.

2.2 Periodic Magnification and Unit Magnification of Moiré Pattern

If the periodic magnification of the moiré pattern generated by the superposition of the microlens array and the micrographics array is M_{period}, it can be defined as the ratio of the periodic size of the moiré pattern to the periodic size of the micrographics array, that is:

$$M_{period} = \frac{S}{d_2} = \frac{max(S_1, S_2, S_3, S_4)}{d_2} \tag{23}$$

Four groups of moiré pattern: moiré pattern 1, moiré pattern 1, moiré pattern 1 and moiré pattern 1 intersect each other to form six new graphics. It is assumed that the areas of the six new graphics are $A_{12}, A_{13}, A_{14}, A_{23}, A_{24}, A_{34}$.

As shown in Fig 13, for the new pattern formed by the intersection of moiré pattern 1 and moiré pattern 2:

$$\overline{AC} * S_1 = \overline{AB} * S_2 = \frac{1}{2}\overline{AC} * \overline{AB} * sin(180^o - \varphi_1 - \varphi_2) \tag{24}$$

Forest Chemicals Revew
www.forestchemicalsreview.com
ISSN: 1520-0191
July-August 2021 Page No. 783-806
Article History: Received: 12 May 2021 Revised: 25 June 2021 Accepted: 22 July 2021 Publication: 31 August 2021

$$\overline{AB} = \frac{2S_1}{sin(180^o - \varphi_1 - \varphi_2)} \tag{25}$$

$$\overline{AC} = \frac{2S_2}{sin(180^o - \varphi_1 - \varphi_2)} \tag{26}$$

From equations (24), (25) and (26), the area A_{12} of the new pattern formed by the intersection of moiré pattern 1 and moiré pattern 2 is:

$$A_{12} = \overline{AB} * \overline{AC} * sin(180^o - \varphi_1 - \varphi_2) = \frac{4S_1S_2}{sin(180^o - \varphi_1 - \varphi_2)} \tag{27}$$

As shown in Fig 14, for the new pattern formed by the intersection of moiré pattern 1 and moiré pattern 3:

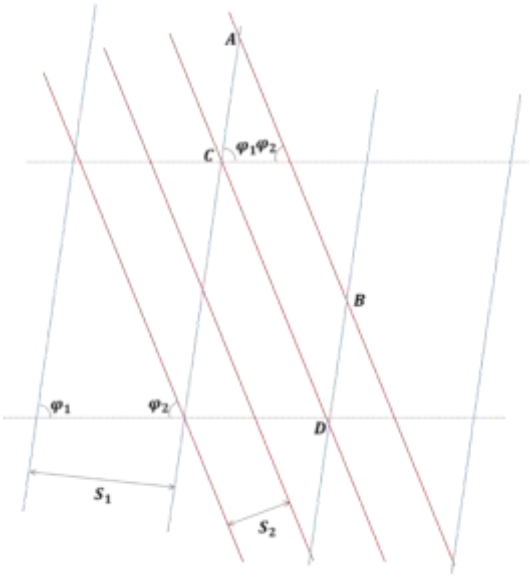

Fig 13: Calculation schematic diagram of a new pattern ABCD formed by the intersection of moiré pattern 1 and moiré pattern 2

Forest Chemicals Revew
www.forestchemicalsreview.com
ISSN: 1520-0191
July-August 2021 Page No. 783-806
Article History: Received: 12 May 2021 Revised: 25 June 2021 Accepted: 22 July 2021 Publication: 31 August 2021

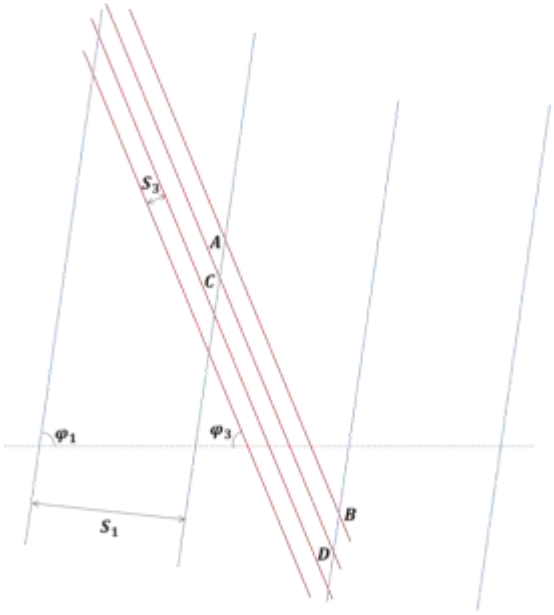

Fig 14: Calculation schematic diagram of a new pattern ABCD formed by the intersection of moiré pattern 1 and moiré pattern 3

$$\overline{AC} * S_1 = \overline{AB} * S_3 = \frac{1}{2}\overline{AC} * \overline{AB} * sin(180^o - \varphi_1 - \varphi_3) \tag{28}$$

$$\overline{AB} = \frac{2S_1}{sin(180^o - \varphi_1 - \varphi_3)} \tag{29}$$

$$\overline{AC} = \frac{2S_3}{sin(180^o - \varphi_1 - \varphi_3)} \tag{30}$$

From equations (28), (29) and (30), the area A_{13} of the new pattern formed by the intersection of moiré pattern 1 and moiré pattern 3 is:

$$A_{13} = \overline{AB} * \overline{AC} * sin(180^o - \varphi_1 - \varphi_3) = \frac{4S_1S_3}{sin(180^o - \varphi_1 - \varphi_3)} \tag{31}$$

As shown in Fig 15, for the new pattern formed by the intersection of moiré pattern 1 and moiré pattern 4:

$$\overline{AC} * S_1 = \overline{AB} * S_4 = \frac{1}{2}\overline{AC} * \overline{AB} * sin(180^o - \varphi_1 - \varphi_4) \tag{32}$$

Forest Chemicals Revew
www.forestchemicalsreview.com
ISSN: 1520-0191
July-August 2021 Page No. 783-806
Article History: Received: 12 May 2021 Revised: 25 June 2021 Accepted: 22 July 2021 Publication: 31 August 2021

$$\overline{AB} = \frac{2S_1}{sin(180^o - \varphi_1 - \varphi_4)} \tag{33}$$

$$\overline{AC} = \frac{2S_4}{sin(180^o - \varphi_1 - \varphi_4)} \tag{34}$$

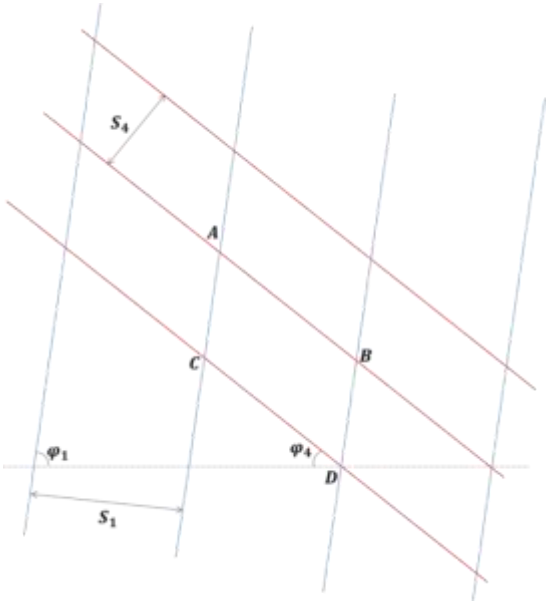

Fig 15: Calculation schematic diagram of a new pattern ABCD formed by the intersection of moiré pattern 1 and moiré pattern 4

From equations (32), (33) and (34), the area A_{14} of the new pattern formed by the intersection of moiré pattern 1 and moiré pattern 4 is:

$$A_{14} = \overline{AB} * \overline{AC} * sin(180^o - \varphi_1 - \varphi_4) = \frac{4S_1S_4}{sin(180^o - \varphi_1 - \varphi_4)} \tag{35}$$

As shown in Fig 16, for the new pattern formed by the intersection of moiré pattern 2 and moiré pattern 3:

$$\overline{AC} * S_2 = \overline{AB} * S_3 = \frac{1}{2}\overline{AC} * \overline{AB} * sin(\varphi_2 - \varphi_3) \tag{36}$$

$$\overline{AB} = \frac{2S_2}{sin(\varphi_2 - \varphi_3)} \tag{37}$$

Forest Chemicals Revew
www.forestchemicalsreview.com
ISSN: 1520-0191
July-August 2021 Page No. 783-806
Article History: Received: 12 May 2021 Revised: 25 June 2021 Accepted: 22 July 2021 Publication: 31 August 2021

$$\overline{AC} = \frac{2S_3}{sin(\varphi_2 - \varphi_3)} \tag{38}$$

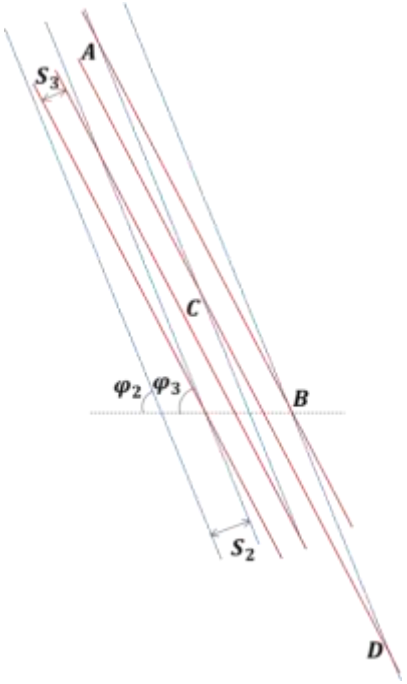

Fig 16: Calculation schematic diagram of a new pattern ABCD formed by the intersection of moiré pattern 2 and moiré pattern 3

From equations (36), (37) and (38), the area A_{23} of the new pattern formed by the intersection of moiré pattern 2 and moiré pattern 3 is:

$$A_{23} = \overline{AB} * \overline{AC} * sin(\varphi_2 - \varphi_3) = \frac{4S_2S_3}{sin(\varphi_2 - \varphi_3)} \tag{39}$$

As shown in Fig 17, for the new pattern formed by the intersection of moiré pattern 2 and moiré pattern 4:

$$\overline{AC} * S_2 = \overline{AB} * S_4 = \frac{1}{2}\overline{AC} * \overline{AB} * sin(\varphi_2 - \varphi_4) \tag{40}$$

$$\overline{AB} = \frac{2S_2}{sin(\varphi_2 - \varphi_4)} \tag{41}$$

Forest Chemicals Revew
www.forestchemicalsreview.com
ISSN: 1520-0191
July-August 2021 Page No. 783-806
Article History: Received: 12 May 2021 Revised: 25 June 2021 Accepted: 22 July 2021 Publication: 31 August 2021

$$\overline{AC} = \frac{2S_4}{sin(\varphi_2 - \varphi_4)} \tag{42}$$

From equations (40), (41) and (42), the area A_{24} of the new pattern formed by the intersection of moiré pattern 2 and moiré pattern 4 is:

$$A_{24} = \overline{AB} * \overline{AC} * sin(\varphi_2 - \varphi_4) = \frac{4S_2S_4}{sin(\varphi_2 - \varphi_4)} \tag{43}$$

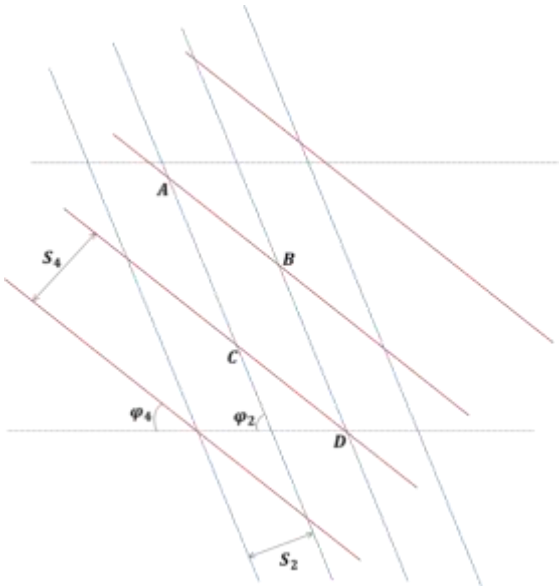

Fig 17: Calculation schematic diagram of a new pattern ABCD formed by the intersection of moiré pattern 2 and moiré pattern 4

Forest Chemicals Revew
www.forestchemicalsreview.com
ISSN: 1520-0191
July-August 2021 Page No. 783-806
Article History: Received: 12 May 2021 Revised: 25 June 2021 Accepted: 22 July 2021 Publication: 31 August 2021

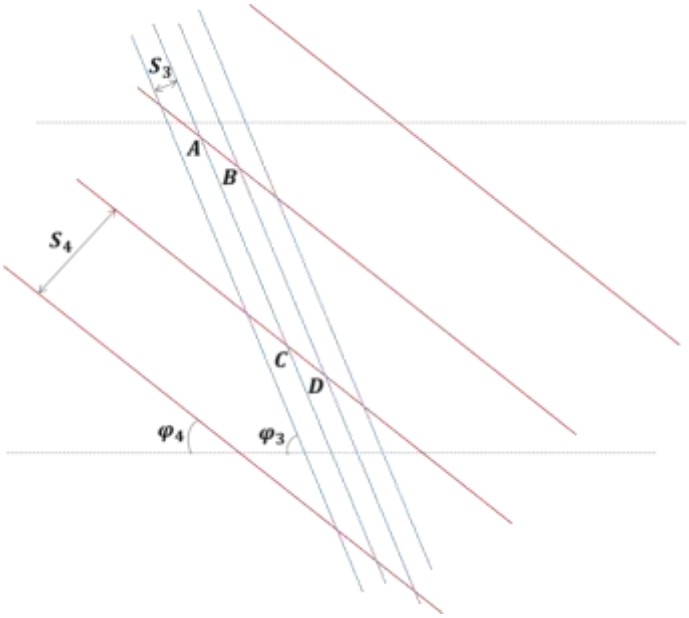

Fig 18: Calculation schematic diagram of a new pattern ABCD formed by the intersection of moiré pattern 3 and moiré pattern 4

As shown in Fig 18, for the new pattern formed by the intersection of moiré pattern 3 and moiré pattern 4:

$$\overline{AC} * S_3 = \overline{AB} * S_4 = \frac{1}{2}\overline{AC} * \overline{AB} * sin(\varphi_3 - \varphi_4) \tag{44}$$

$$\overline{AB} = \frac{2S_3}{sin(\varphi_3 - \varphi_4)} \tag{45}$$

$$\overline{AC} = \frac{2S_4}{sin(\varphi_3 - \varphi_4)} \tag{46}$$

From equations (44), (45) and (46), the area A_{34} of the new pattern formed by the intersection of moiré pattern 3 and moiré pattern 4 is:

$$A_{34} = \overline{AB} * \overline{AC} * sin(\varphi_3 - \varphi_4) = \frac{4S_3S_4}{sin(\varphi_3 - \varphi_4)} \tag{47}$$

If the area of the micrographics array unit is A_{unit} and the unit magnification of the moiré pattern generated by the superposition of the microlens array and the micrographics array is

Forest Chemicals Revew
www.forestchemicalsreview.com
ISSN: 1520-0191
July-August 2021 Page No. 783-806
Article History: Received: 12 May 2021 Revised: 25 June 2021 Accepted: 22 July 2021 Publication: 31 August 2021

M_{unit}, M_{unit} can be defined as the maximum value of the area ratio of the area of the six new graphics to the area of the micrographics array unit, that is:

$$M_{unit} = max\left(\frac{A_{12}}{A_{unit}}, \frac{A_{13}}{A_{unit}}, \frac{A_{14}}{A_{unit}}, \frac{A_{23}}{A_{unit}}, \frac{A_{24}}{A_{unit}}, \frac{A_{34}}{A_{unit}}\right) \quad (48)$$

III. COMPARISON OF THEORETICAL AND EXPERIMENTAL RESULTS OF MOIRE PATTERN DISPLAY

This section describes the normal structure of a manuscript and how each part should be handled. In this section, UV-LED nanoimprinting process and UV offset printing process based on PS plate were used to manufacture 3D printed matter integrating microlens array and micrographics array. The microlens array is hexagonal aperture and honeycomb arrangement, and the micrographics array is circular aperture and honeycomb arrangement. The manufacturing process parameters: the imprinting speed was 7 *m / min*; the printing speed was 30 *m / h*, the printing pressure was 0.01 *Pa* [1][19].

In order to verify the effectiveness of theoretical analysis method of moiré display based on microlens array in Section 2, two typical cases were selected, in which the microlens array period d_1, micrographics array period d_2 and the superposition angle θ of 3D printed matter met the following requirements:

In the first case, the period of the micrographics array is slightly less than that of the microlens array, assuming that $d_1 = 70\,um, d_2 = 69\,um$, and the superposition angles are $0^o, 30^o, 60^o, 90^o$ respectively.

In the second case, the period of the micrographics array is slightly larger than that of the microlens array, assuming that $d_1 = 70\,um, d_2 = 71\,um$, and the superposition angles are $0^o, 30^o, 60^o, 90^o$ respectively.

In both cases, the radius of micrographics unit is assumed to be $30\,um$.

For the convenience of expression, the mathematical relationship between period S_φ, direction angle φ, periodic magnification M_{period}, unit magnification M_{unit} of moiré pattern and microlens array period d_1, micrographics array d_2 and their superposition angle θ in section 2 can be expressed as follows:

Forest Chemicals Revew
www.forestchemicalsreview.com
ISSN: 1520-0191
July-August 2021 Page No. 783-806
Article History: Received: 12 May 2021 Revised: 25 June 2021 Accepted: 22 July 2021 Publication: 31 August 2021

$$\begin{aligned} S_\varphi &= f_1(d_1, d_2, \theta) \\ \varphi &= f_2(d_1, d_2, \theta) \\ M_{period} &= f_3(d_1, d_2, \theta) \\ M_{unit} &= f_4(d_1, d_2, \theta) \end{aligned} \tag{49}$$

According to the mathematical relationship in Section 2 (as equation 49), the theoretical values of period S_φ, direction angle φ, periodic magnification M_{period} and unit magnification M_{unit} of moiré pattern in the above two cases were calculated respectively, as shown in TABLE I.

TABLE I. Theoretical Values of Period S_φ, Direction Angle φ, Periodic Magnification M_{period} and Unit Magnification M_{unit} of Moiré Pattern in the Two Cases

SERIAL NUMBER	PERIOD S_φ	DIRECTION ANGLE φ	PERIODIC MAGNIFICATION M_{period}	UNIT MAGNIFICATION M_{unit}
Case 1($\boldsymbol{\theta = 0^o}$)	4830 *um*	0^o	70	38109
Case 1($\boldsymbol{\theta = 30^o}$)	134 *um*	77^o	2	274
Case 1($\boldsymbol{\theta = 60^o}$)	4830 *um*	0^o	70	552
Case 1($\boldsymbol{\theta = 90^o}$)	134 *um*	77^o	2	274
Case 2($\boldsymbol{\theta = 0^o}$)	4970 *um*	0^o	70	40351
Case 2($\boldsymbol{\theta = 30^o}$)	136 *um*	73^o	2	286
Case 2($\boldsymbol{\theta = 60^o}$)	4970 *um*	0^o	70	576
Case 2($\boldsymbol{\theta = 90^o}$)	136 *um*	73^o	2	286

The experimental values of period S_φ, direction angle φ, periodic magnification M_{period} and unit magnification M_{unit} of moiré pattern in the above two cases were measured by the laser confocal microscope, as shown in TABLE II.

TABLE II. Experimental Values of Period S_φ, Direction Angle φ, Periodic Magnification M_{period} and Unit Magnification M_{unit} of Moiré Pattern in the Two Cases

Forest Chemicals Revew
www.forestchemicalsreview.com
ISSN: 1520-0191
July-August 2021 Page No. 783-806
Article History: Received: 12 May 2021 Revised: 25 June 2021 Accepted: 22 July 2021 Publication: 31 August 2021

SERIAL NUMBER	PERIOD S_φ	DIRECTION ANGLE φ	PERIODIC MAGNIFICATION M_{period}	UNIT MAGNIFICATION M_{unit}
Case 1($\boldsymbol{\theta = 0^o}$)	4825	0^o	70	—
Case 1($\boldsymbol{\theta = 30^o}$)	133	76^o	2	276
Case 1($\boldsymbol{\theta = 60^o}$)	4827	0^o	70	550
Case 1($\boldsymbol{\theta = 90^o}$)	132	76^o	2	273
Case 2($\boldsymbol{\theta = 0^o}$)	4974	0^o	70	—
Case 2($\boldsymbol{\theta = 30^o}$)	135	74^o	2	284
Case 2($\boldsymbol{\theta = 60^o}$)	4966	0^o	70	579
Case 2($\boldsymbol{\theta = 90^o}$)	138	74^o	2	288

Calculate the deviation rate between the experimental value and the theoretical value in two cases, as shown in TABLE III.

TABLE III. Deviation Rates of Experimental and Theoretical Values of Period S_φ, Direction Angle φ, Periodic Magnification M_{period} and Unit Magnification M_{unit} of Moiré Pattern in Two Cases

SERIAL NUMBER	PERIOD S_φ	DIRECTION ANGLE φ	PERIODIC MAGNIFICATION M_{period}	UNIT MAGNIFICATION M_{unit}
Case 1($\boldsymbol{\theta = 0^o}$)	0.10%	0	0	—
Case 1($\boldsymbol{\theta = 30^o}$)	0.75%	1.30%	0	0.73%
Case 1($\boldsymbol{\theta = 60^o}$)	0.06%	0	0	0.36%
Case 1($\boldsymbol{\theta = 90^o}$)	1.50%	1.30%	0	0.36%
Case 2($\boldsymbol{\theta = 0^o}$)	0.08%	0	0	—
Case 2($\boldsymbol{\theta = 30^o}$)	0.74%	1.37%	0	0.70%
Case 2($\boldsymbol{\theta = 60^o}$)	0.08%	0	0	0.52%
Case 2($\boldsymbol{\theta = 90^o}$)	1.47%	1.37%	0	0.70%

As can be seen from TABLE III, the deviation rates of experimental and theoretical values of period S_φ, direction angle φ, periodic magnification M_{period} and unit magnification M_{unit} of moiré pattern in two cases are all less than 2%, which verifies the effectiveness of the theoretical analysis method of moiré display based on microlens array in Section 2.

Forest Chemicals Revew
www.forestchemicalsreview.com
ISSN: 1520-0191
July-August 2021 Page No. 783-806
Article History: Received: 12 May 2021 Revised: 25 June 2021 Accepted: 22 July 2021 Publication: 31 August 2021

IV. CONCLUSION

In this paper, on the basis of the existing geometric transformation method, a theoretical analysis method of moiré display was proposed for microlens array with regular hexagonal aperture and honeycomb arrangement, which gave consideration to the imaging characteristics of moiré pattern, such as periodic amplification, unit amplification and spatial direction. The mathematical relationship between the period, direction angle, period magnification, unit magnification of moiré pattern and the period of microlens array, the period of micrographics array, as well as the superposition angle of them were derived in detail. The two typical cases were selected, and the theoretical and experimental values of the period, the direction angle, the period magnification and the unit magnification of moiré pattern were calculated and tested respectively. The differences between the theoretical and experimental values were then compared. The results show that the deviation rates between the experimental and theoretical values of the period, the direction angle, the period magnification and the unit magnification are all less than 2% in two typical cases, which verified the effectiveness of the proposed moiré display theoretical analysis method.

ACKNOWLEDGEMENTS

This research was supported by a grant from the Department of Education of Guangdong Province (“The study of cross-media color reproduction system based on HDRI multi-spectral technology”, NO. 6020210017K).

REFERENCES

[1] Chen LY (2020) Research on naked-eye 3D printing technology based on microlens array. South China University of Technology
[2] Hutley MC, Hunt R, Stevens RF (1994) The moiré magnifier. Pure Applied Optics 3(2):133
[3] Stevens RF (1999) Optical inspection of periodic structures using lens arrays and moiré magnification. The Imaging Science Journal 47(4):173-179
[4] Cadarso VJ, Chosson S, et al. (2013) High-resolution 1D moirés as counterfeit security features. Light: Science & Applications 2(7):1-5
[5] Yu XB, Sang XZ, et al. (2015) Large viewing angle three-dimensional display with smooth motion parallax and accurate depth cues. Optics Express 23(20):25950-25958
[6] Huang P, He CW, et al. (2018) Properties of dynamic image displacements based on microstructure. Applied Optics 57(28):8187-8192

Forest Chemicals Revew
www.forestchemicalsreview.com
ISSN: 1520-0191
July-August 2021 Page No. 783-806
Article History: Received: 12 May 2021 Revised: 25 June 2021 Accepted: 22 July 2021 Publication: 31 August 2021

[7] Ouyang CB, LiuG, et al. (2019) Design and analysis method of moiré magnifier based on depth cues from disparity. Optoelectronics Letters 15(4):255-259
[8] Zheng WW, ShenS, et al. Design methodology for moiré magnifier based on micro-focusing elements. Optics Express 25(25):31746-31757
[9] YuJ, Zheng WW, et al. Dynamic effect in moiré magnifier by using of weak domain transformation. Optics Express 28(8):11065-11073
[10] Huang P, He CW, et al. (2020) Superposition of micropattern and microlens arrays for improved dynamic moiré pattern. Physica Scripta 95(5):055002
[11] Amidror I (2007) The theory of the moiré phenomenon. 2nd ed. Springer Netherlands
[12] Yin GK (2015) Theory and experiment of moiré display based on the square-aperture planar microlens array. Southwest University
[13] Zhang BH (2016) Investigations on the Talbot effect and moiré effect of the square -aperture microlens array. Southwest University
[14] Zheng SC (2018) Theory and experiment of micro-angle measurement based on two-dimensional moiré fringes generated by square aperture microlens array. Southwest University
[15] Xu X (2020) Theory and experiment of micro-angle measurement based on two-dimensional Talbot-moiré effect. Southwest University
[16] Amidror I Hersch RD (2010) Mathematical moiré models and their limitations. Journal of Modern Optics 57(1):23-36
[17] Amidror I (1994) Spectral analysis and minimization of moiré patterns in color separation. Journal of Electronic Imaging 3(3):295-317
[18] Amidror I, Hersch RD (2009) The role of Fourier theory and of modulation in the prediction of visible moiré effect. Journal of Modern Optics 56(9):1103-1118
[19] Chen LY, Chen GX, et al. (2020) Naked-eye 3D display based on microlens array using combined micro-nano imprint and UV offset printing methods. Molecules 25(9):1-16